

Activation of entanglement from quantum coherence and superposition

Lu-Feng Qiao,^{1,2,*} Jun Gao,^{1,2,*} Alexander Streltsov,^{3,4,*} Swapan Rana,⁵ Ruo-Jing Ren,^{1,2}
Zhi-Qiang Jiao,^{1,2} Cheng-Qiu Hu,^{1,2} Xiao-Yun Xu,^{1,2} Ci-Yu Wang,^{1,2} Hao Tang,^{1,2}
Ai-Lin Yang,^{1,2} Zhi-Hao Ma,⁶ Maciej Lewenstein,^{5,7} and Xian-Min Jin^{1,2,†}

¹State Key Laboratory of Advanced Optical Communication Systems and Networks,
Institute of Natural Sciences & Department of Physics and Astronomy,
Shanghai Jiao Tong University, Shanghai 200240, China

²Synergetic Innovation Center of Quantum Information and Quantum Physics,
University of Science and Technology of China, Hefei, Anhui 230026, China

³Faculty of Applied Physics and Mathematics, Gdańsk University of Technology, 80-233 Gdańsk, Poland

⁴National Quantum Information Centre in Gdańsk, 81-824 Sopot, Poland

⁵ICFO – Institut de Ciències Fotoniques, The Barcelona Institute of Science and Technology, ES-08860 Castelldefels, Spain

⁶Department of Mathematics, Shanghai Jiaotong University, Shanghai 200240, China

⁷ICREA, Pg. Lluis Companys 23, ES-08010 Barcelona, Spain

Quantum entanglement and coherence are two fundamental features of nature, arising from the superposition principle of quantum mechanics [1]. While considered as puzzling phenomena in the early days of quantum theory [2], it is only very recently that entanglement and coherence have been recognized as resources for the emerging quantum technologies, including quantum metrology, quantum communication, and quantum computing [3, 4]. In this work we study the limitations for the interconversion between coherence and entanglement. We prove a fundamental no-go theorem, stating that a general resource theory of superposition does not allow for entanglement activation. By constructing a CNOT gate as a free operation, we experimentally show that such activation is possible within the more constrained framework of quantum coherence. Our results provide new insights into the interplay between coherence and entanglement, representing a substantial step forward for solving longstanding open questions in quantum information science.

Quantum resource theories provide a fundamental framework for studying general notions of nonclassicality, including quantum entanglement [3, 5] and coherence [4, 6]. Any such resource theory is based on the notion of free states and free operations. Free operations are physical transformations which do not consume any resources. They strongly depend on the problem under study, and are usually motivated by physical or technological constraints. In entanglement theory, these constraints are naturally given by the *distance lab paradigm*: two spatially separated parties can perform quantum measurements in their local labs, but can only exchange classical information between each other.

Free states of a resource theory are quantum states which can be produced without consuming any resources. In entanglement theory, these free states are called separable [7]. Various quantum protocols require the presence of entanglement. This includes quantum

teleportation [8, 9], quantum cryptography [10], and quantum state merging [11]. As has been demonstrated very recently, it is indeed possible to establish and maintain high degree of entanglement via large distances [12].

The resource theory of quantum coherence studies technological limitations for establishing quantum superpositions [4, 6]. This theory requires the existence of a distinguished basis, which can be interpreted as *classical*, and is usually present due to the unavoidable decoherence [13]. Quantum states belonging to this basis are then called incoherent, and considered as the free states of coherence theory. Superpositions of these free states are said to possess coherence. Incoherent operations are free operations of coherence theory: they correspond to quantum measurements which do not create coherence for individual measurement outcomes [6]. Recent results show that coherence plays a crucial role for quantum metrology [14, 15], and that coherence might be more suitable than entanglement to capture the performance of quantum algorithms [16, 17]. Recent investigations also show that coherence and entanglement play an important role in biological systems [18].

Due to the aforementioned significance of coherence and entanglement for quantum technologies, it is crucial to understand how these fundamental resources can be converted into each other. In this work we address this question, and confirm our theoretical results by an experiment with photons. We present a fundamental no-go theorem, showing that a general resource theory of superposition does not allow for entanglement activation, while this is possible within the more constrained theory of coherence. This result shares the same spirit with the celebrated no-cloning theorem [19]: a general quantum state cannot be copied, while cloning is in fact possible for a restricted set of mutually orthogonal states. We experimentally demonstrate entanglement activation from coherence by preparing photon states with different degrees of coherence and activating them into entanglement by applying an optical CNOT gate. Our results

lead to a fundamental insight about entanglement quantifiers, proving that trace norm entanglement violates strong monotonicity. This shows how recent results on the resource theory of quantum coherence can be used for solving important open questions in quantum information science.

NO-GO THEOREM OF ENTANGLEMENT ACTIVATION

Entanglement activation from coherence has been first studied in [20]. There, it was shown that any nonzero amount of coherence in a quantum state ρ can be activated into entanglement by coupling the state to an incoherent ancilla σ_i and performing a bipartite incoherent operation on the total state $\rho \otimes \sigma_i$. On a quantitative level, the amount of coherence in a state ρ bounds the amount of activated entanglement as [20]

$$E(\Lambda_i[\rho \otimes \sigma_i]) \leq C(\rho), \quad (1)$$

where Λ_i is an incoherent operation, and E and C are general distance-based entanglement and coherence monotones, see Methods section for rigorous definitions and more details. In many relevant cases, the optimal incoherent operation saturating the inequality (1) is the CNOT gate (see Fig. 1).

We will now study this relation from a very general perspective, by resorting to the resource theory of superposition [21, 22]. In this theory, the free states $\{|c_i\rangle\}$ are not necessarily mutually orthogonal. Thus, the theory of superposition is more general than the resource theory of coherence, and is indeed powerful enough to cover also the resource theory of entanglement, which is obtained by allowing for continuous sets of free states. Any convex combination of the free states $\{|c_i\rangle\}$ is also a free state, which is a very natural assumption in any quantum resource theory. Free operations and further properties of the resource theory of superposition have been discussed in [21, 22].

In the following we will study the resource theory of superposition for a two-qubit system. We assume that each of the qubits has two pure free states which we denote by $|c_0\rangle$ and $|c_1\rangle$, assuming that $0 < |\langle c_0|c_1\rangle| < 1$. Pure free states of both qubits have the form $|c_i\rangle \otimes |c_j\rangle$, and convex combinations of such states are also free. We will now consider unitary operations which do not create superpositions of the free states on both qubits. Following the notion of Ref. [22], we will call these unitaries *superposition-free*. In general, these unitaries induce the transformation

$$U |c_k\rangle |c_l\rangle = e^{i\phi_{kl}} |c_m\rangle |c_n\rangle \quad (2)$$

with some phases $e^{i\phi_{kl}}$. Our main question in this context is the following: *can a bipartite superposition-free unitary*

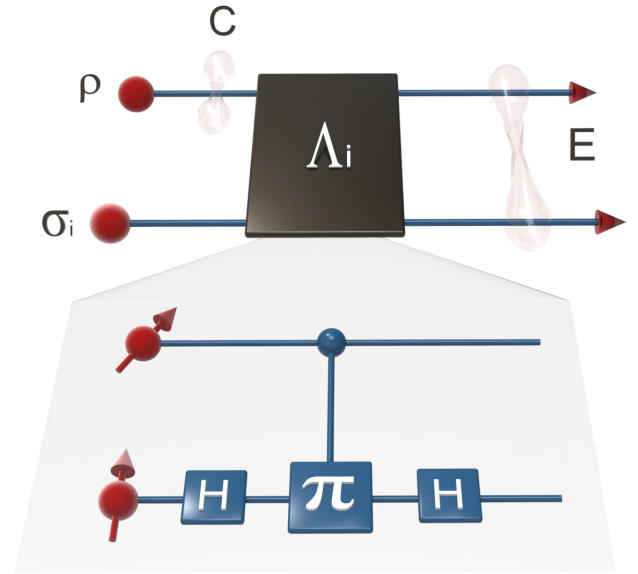


Figure 1. **The conceptual graph of the conversion process.** Two individual quantum states are generated and labeled as the system state and the ancilla state, respectively. The system state ρ is prepared with a nonzero amount of coherence $C(\rho)$, while the ancilla is initialized in an incoherent state σ_i . After an incoherent operation Λ_i acting on the system and ancilla, the two-qubit state is either entangled or separable, depending on whether the initial system state ρ has coherence or not. Here, we choose the CNOT gate as the optimal incoherent operation, which is decomposed into one controlled phase gate and two Hadamard gates.

create entanglement? The answer to this question is affirmative in the traditional framework of quantum coherence, i.e., for orthogonal free states $|c_0\rangle$ and $|c_1\rangle$ [20]. In this case, the CNOT gate is a superposition-free unitary which can create entanglement. It is reasonable to believe that these ideas transfer to the more general concept of superpositions, and that superposition-free unitaries also allow to create entanglement.

Quite surprisingly, we will see in the following that this is not the case for the framework considered here. This is the statement of the following theorem.

Theorem 1. *It is not possible to create entanglement via superposition-free unitaries on two qubits.*

We note that the theorem applies for the case where each of the qubits has two superposition-free states $|c_0\rangle$ and $|c_1\rangle$ with $0 < |\langle c_0|c_1\rangle| < 1$. The proof of this theorem will be a combination of several results, which we will present below.

Before we prove the above theorem, we will first show that every superposition-free unitary on two qubits can be decomposed into two elementary operations, which we will denote by V and W . The first elementary operation is the swap gate $V = \sum_{i,j} |ij\rangle\langle ji|$, which corresponds

Unitary	V^2	V	WVW	$(VW)^2$	W	WV	VWV	VW
$e^{i\phi_{00}}$	1	1	1	1	1	1	1	1
$e^{i\phi_{11}}$	1	1	$\frac{\langle c_0 c_1\rangle^2}{\langle c_1 c_0\rangle^2}$	$\frac{\langle c_0 c_1\rangle^2}{\langle c_1 c_0\rangle^2}$	$\frac{\langle c_0 c_1\rangle}{\langle c_1 c_0\rangle}$			
$e^{i\phi_{01}}$	1	1	$\frac{\langle c_0 c_1\rangle}{\langle c_1 c_0\rangle}$	$\frac{\langle c_0 c_1\rangle}{\langle c_1 c_0\rangle}$	1	$\frac{\langle c_0 c_1\rangle}{\langle c_1 c_0\rangle}$	$\frac{\langle c_0 c_1\rangle}{\langle c_1 c_0\rangle}$	1
$e^{i\phi_{10}}$	1	1	$\frac{\langle c_0 c_1\rangle}{\langle c_1 c_0\rangle}$	$\frac{\langle c_0 c_1\rangle}{\langle c_1 c_0\rangle}$	$\frac{\langle c_0 c_1\rangle}{\langle c_1 c_0\rangle}$	1	1	$\frac{\langle c_0 c_1\rangle}{\langle c_1 c_0\rangle}$

Table I. **All superposition-free unitaries on two qubits.** Any superposition-free unitary on two qubits can be expressed as a product of elementary unitaries V and W given in the main text. The phases $e^{i\phi_{kl}}$ in the table correspond to the phases in Eq. (2).

to an exchange of the two qubits:

$$V|c_k\rangle|c_l\rangle \rightarrow |c_l\rangle|c_k\rangle. \quad (3)$$

The second elementary operation transforms an initial superposition-free state $|c_k\rangle|c_l\rangle$ as follows:

$$W|c_k\rangle|c_l\rangle = e^{i\phi_k}|c_{\text{mod}(k+1,2)}\rangle|c_l\rangle, \quad (4)$$

where the phases $e^{i\phi_k}$ are defined as

$$e^{i\phi_0} = 1, \quad e^{i\phi_1} = \frac{\langle c_0|c_1\rangle}{\langle c_1|c_0\rangle}. \quad (5)$$

The existence of such a unitary is guaranteed by Lemma 3 in [23] (see also [21, 24]). Note that Eq. (4) defines the action of W onto any pure two-qubit state $|\psi\rangle$, since any such state can be written as $|\psi\rangle = \sum_{k,l} a_{kl}|c_k\rangle|c_l\rangle$ with complex numbers a_{kl} . Moreover, W can be chosen to be a local unitary, acting on the first qubit only. With these tools, we are now in position to prove the following theorem.

Theorem 2. *There exist only eight superposition-free unitaries for two qubits, which can all be expressed as combinations of V and W .*

This theorem applies to the same framework of superposition as Theorem 1, i.e., it holds if each qubit has two superposition-free states $|c_0\rangle$ and $|c_1\rangle$ with $0 < |\langle c_0|c_1\rangle| < 1$. The proof of the theorem is given in Appendix A. We list all eight possible transformations in Table I.

The tools provided so far give important insight on the structure of superposition-free unitaries for two qubits and allow us to complete the proof of Theorem 1. For this, it is enough to show that both elementary operations V and W cannot create entanglement. Clearly, entanglement cannot be created with the swap unitary V . The second elementary operation W also cannot create entanglement, as it can be implemented as a local unitary acting on the first qubit only.

At this point it is interesting to compare our results to results reported in [21, 25]. Applied to the setting considered here, the results of [21] imply that superposition can be converted into entanglement in a *universal* way: there exists a (not necessarily superposition-free)

quantum operation Λ which universally converts any state of the form $|\psi\rangle = (\alpha_0|c_0\rangle + \alpha_1|c_1\rangle) \otimes |c_0\rangle$ into an entangled state whenever both coefficients α_0 and α_1 are nonzero. Note that this is not a contradiction to our results presented above, as the quantum operation Λ in this conversion is not necessarily superposition-free.

We will now show how recent advances in coherence theory can be used to solve important open questions in the theory of entanglement. For this, we recall that Eq. (1) also applies to entanglement and coherence quantifiers based on the trace norm:

$$C_t(\rho) = \min_{\sigma \in \mathcal{I}} \|\rho - \sigma\|_1, \quad (6)$$

$$E_t(\rho) = \min_{\sigma \in \mathcal{S}} \|\rho - \sigma\|_1, \quad (7)$$

where \mathcal{I} and \mathcal{S} are the sets of incoherent and separable states, respectively. The trace norm $\|M\|_1 = \text{Tr} \sqrt{M^\dagger M}$ is one of the most important quantities in quantum information theory. Its significance comes from its operational interpretation, as $p = 1/2 + \|\rho - \sigma\|_1/4$ is the optimal probability for distinguishing two quantum states ρ and σ via quantum measurements. The coherence and entanglement quantifiers (6) and (7) thus have the operational interpretation via the probability to distinguish a state ρ from the set of incoherent and separable states, respectively.

Despite its clear operational significance, it is only very recently that the trace norm has been investigated within the resource theory of quantum coherence [26–28], and surprisingly little is known about the trace norm entanglement E_t [29]. Remarkably, it was shown in [28] that C_t violates strong monotonicity: the trace norm coherence of a state can increase on average under a suitable incoherent operation. We refer to the Methods section for a rigorous definition of strong monotonicity. As we show in the following theorem, these results also extend to the trace norm entanglement, thus settling an important question in entanglement theory which was open for decades.

Theorem 3. *Trace norm entanglement is not a strong entanglement monotone.*

The proof of the theorem can be found in Appendix B, where we in fact show that the trace norm entanglement can increase on average under a local measurement. This finishes the theoretical part of this work, and we will now focus on experimental entanglement activation from coherence.

EXPERIMENTAL ENTANGLEMENT ACTIVATION FROM COHERENCE

The results presented above impose strong constraints on the possible activation of superpositions into entanglement. On the other hand, it is known that activation

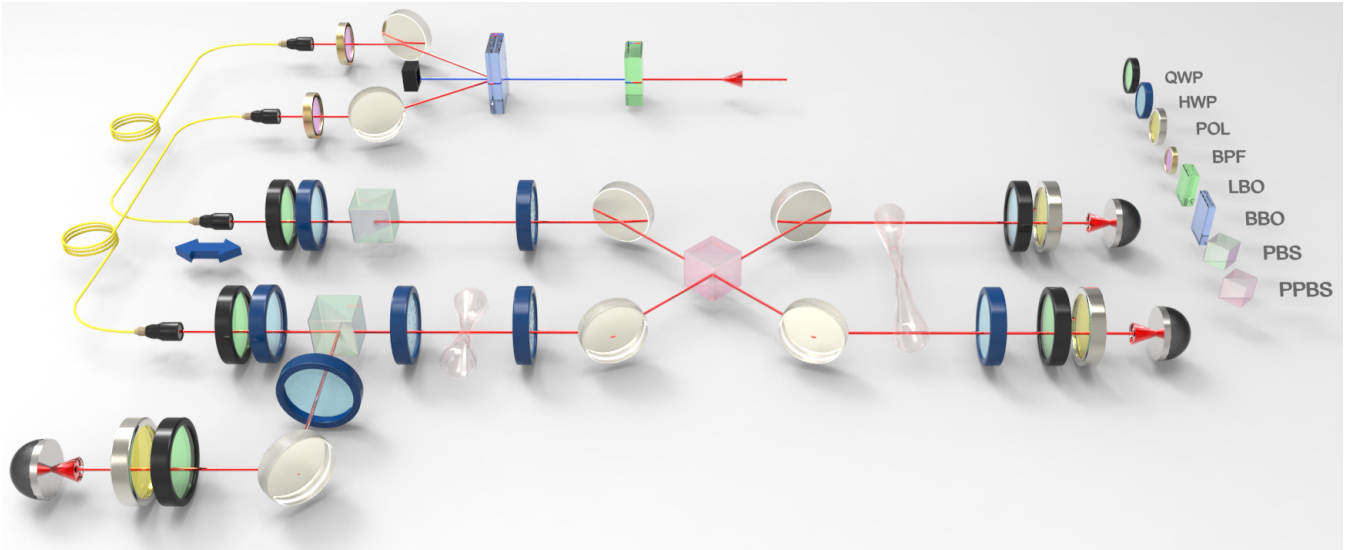


Figure 2. **Experimental setup.** Pairs of identical photons are generated via type-II spontaneous parametric down-conversion process in a BBO crystal by a 390nm UV laser up-converted from a mode lock Ti:sapphire oscillator. After passing the 3nm band pass filter (BPF), the photon pairs are coupled into the single mode fibers and launched to the incoherent operation section. A quarter wave plate (QWP) and a half wave plate (HWP) are used for polarization compensation. A combination of HWPs and a partial polarizing beam splitter (PPBS) acts as the incoherent operation. The system states are prepared with different amount of coherence by rotating a HWP following of the PBS. The two-qubit states and an additional copy of the system states are analyzed by quantum state tomography.

of entanglement from *coherence* is possible [20], i.e., the aforementioned constraints can be circumvented if the free states $|c_0\rangle$ and $|c_1\rangle$ are orthogonal. In this case, as is shown in Fig. 1, any nonzero amount of coherence in a state ρ can be converted into entanglement by adding an incoherent ancilla σ_i and performing a bipartite incoherent unitary on the total state $\rho \otimes \sigma_i$. As we will see in the following, such an activation can indeed be performed with current experimental techniques.

Following our previous discussion, the individual systems will be qubits. As a quantifier of coherence we will use the ℓ_1 -norm of coherence, which is a strong coherence monotone, and corresponds to the sum of the absolute values of the off-diagonal elements [6]:

$$C(\rho) = \sum_{i \neq j} |\rho_{ij}|. \quad (8)$$

After performing a bipartite incoherent operation on the total state $\rho \otimes \sigma_i$, the amount of entanglement in the total state will be quantified via concurrence E . Concurrence is a natural entanglement quantifier for two-qubit states, as it admits the following closed expression [30]:

$$E(\rho) = \max\{0, \lambda_1 - \lambda_2 - \lambda_3 - \lambda_4\}, \quad (9)$$

where λ_i are the square roots of the eigenvalues of $\rho \tilde{\rho}$ in decreasing order, and $\tilde{\rho}$ is defined as $\tilde{\rho} = (\sigma_y \otimes \sigma_y) \rho^* (\sigma_y \otimes \sigma_y)$ with Pauli y -matrix σ_y , and complex conjugation is taken in the computational basis.

As we show in Appendix C, Eq. (1) also applies in this situation, i.e., the amount of coherence in the state ρ bounds the amount of concurrence that can be activated from the state via incoherent operations. Moreover, the optimal incoherent operation in the above setting is the CNOT gate, as it allows to saturate the inequality (1). We also note that for the systems considered here the ℓ_1 -norm coherence coincides with the trace norm coherence [31]. Thus, the results discussed in this section also hold if C is the trace norm coherence defined in Eq. (6).

Here, we experimentally verify this relation between coherence and entanglement by the means of quantum optics, using the fact that polarization is easy to manipulate with high precision. By utilizing the phase flip

ZZ	$ \langle 00 $	$ \langle 01 $	$ \langle 10 $	$ \langle 11 $
$ 00\rangle$	0.929	0.034	0.033	0.004
$ 01\rangle$	0.053	0.914	0.002	0.031
$ 10\rangle$	0.004	0.002	0.159	0.835
$ 11\rangle$	0.001	0.005	0.816	0.178
XX	$ \langle 00 $	$ \langle 01 $	$ \langle 10 $	$ \langle 11 $
$ 00\rangle$	0.896	0.004	0.099	0.001
$ 01\rangle$	0.002	0.173	0.001	0.824
$ 10\rangle$	0.103	0.002	0.892	0.003
$ 11\rangle$	0.001	0.827	0.001	0.171

Table II. Truth table of the CNOT gate.

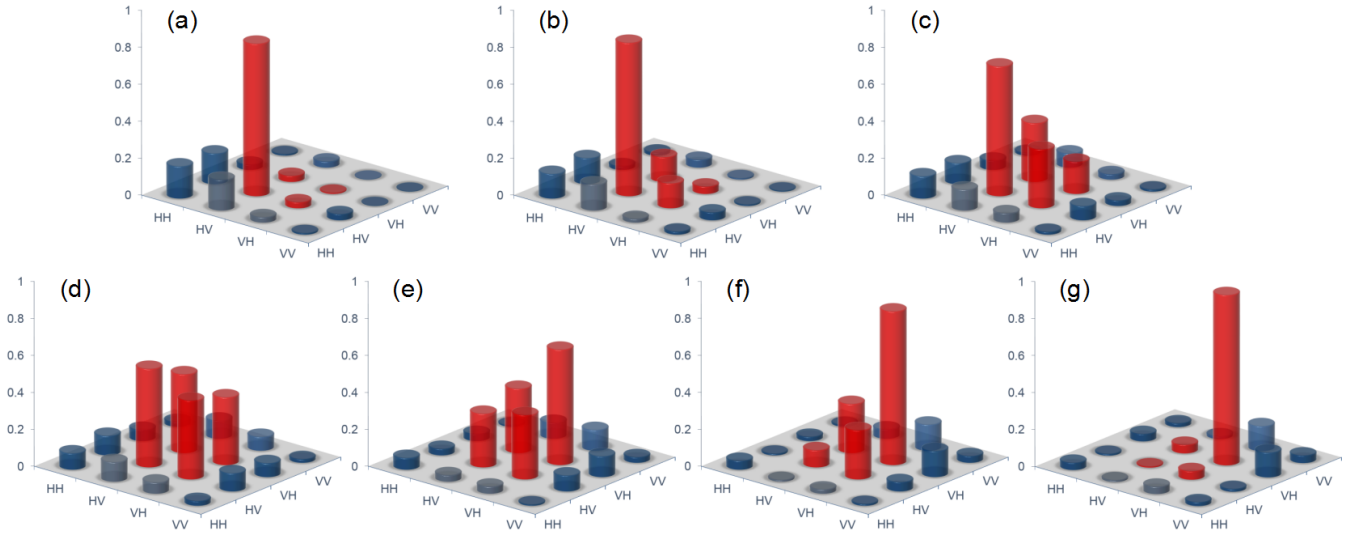


Figure 3. **Experimental results of two-qubit tomography.** The density matrices with different system states $\cos(\vartheta)|H\rangle + \sin(\vartheta)|V\rangle$ as the input state by scanning different polarizations (a) $\vartheta = 0^\circ$; (b) $\vartheta = 15^\circ$; (c) $\vartheta = 30^\circ$; (d) $\vartheta = 45^\circ$; (e) $\vartheta = 60^\circ$; (f) $\vartheta = 75^\circ$; (g) $\vartheta = 90^\circ$. From (a) to (d), it is obvious that the generated entangled states vary from separable states to maximal entangled state while from (e) to (g), the entanglement gradually decreases due to the decline of the coherence.

introduced by second order interference, we construct the incoherent operation with a combination of a controlled phase gate and two Hadamard gates. We prepare a set of system states with different amount of coherence, and observe that coherence and entanglement are highly correlated with acceptable errors under the state of art of optical CNOT operation [32–34].

The sketch of our experiment setup is shown in Fig. 2. It can be divided into three parts: the preparation of identical photons, the incoherent operation and the state analysis module. We use a mode lock Ti:sapphire oscillator emitting 130fs pulses centered at 780nm with a repetition rate of 77MHz. The near-infrared light is frequency doubled to ultraviolet light of 390nm in a 1.3mm thick LiB_3O_5 (LBO) crystal. Two identical photons are created by pumping a 2mm thick $\beta-BaB_2O_4$ (BBO) crystal via a type-II spontaneous parametric down-conversion process in a beam-like scheme [35, 36]. Two 3nm band pass filters are used to improve the visibility of interference for it ensures the spectral indistinguishability of the photon pairs. The photons are coupled into the single mode fibers, with one serving as the system photon while the other one as the ancilla photon. A quarter wave plate and a half wave plate are used in both arms to compensate the polarization rotation induced by the single mode fibers.

The two indistinguishable photons are then injected into the CNOT gate module based on the second-order interference [37]. The key feature in this optical CNOT gate scheme is a partial polarizing beam splitter (PPBS), which perfectly reflects vertical polarization and reflects (transmits) 1/3 (2/3) of horizontal polarization. We mount the coupler for the ancilla photon on a one-

dimensional translation stage to ensure the temporal overlap between the photon pairs. The ideal HOM interference visibility on this PPBS is $V_{th} = 80\%$ and we experimentally achieve $V_{exp} = 67.9 \pm 1.0\%$. The relative visibility is $V_{re} = V_{exp}/V_{th} = 84.9\%$. The mismatch can be attributed to the imperfection of the PPBS, whose reflection ratio of the horizontal polarization 29% deviates from the ideal value of 33.3. In order to evaluate the performance of the CNOT gate, we measure the truth tables and estimate the process fidelity [38]. In the ZZ basis, we define the computational basis as $|0\rangle_z = |H\rangle$ and $|1\rangle_z = |V\rangle$ for the control qubit and $|0\rangle_z = |D\rangle$ and $|1\rangle_z = |A\rangle$ for the target qubit. The CNOT gate flips the target qubit when the control qubit is $|1\rangle_z$. In the XX basis, it is equivalent to transform the bases using a Hadamard gate, where the control qubit is encoded in $|D\rangle - |A\rangle$ basis and the target qubit in $|H\rangle - |V\rangle$ basis. Table II gives the normalized possibilities of all the combinations with four different input and output states in both ZZ and XX basis. We can see that the control and the target qubit swap in the XX basis, where the control qubit remains unchanged when the target qubit is $|0\rangle_x$ and flips when the target qubit is $|1\rangle_x$.

The fidelity can be defined as the average value of the possibility to get the correct output over all inputs. From this definition we can calculate $F_{zz} = 0.87$ and $F_{xx} = 0.86$. These two complementary fidelity values can bound the quantum process fidelity according to [38]

$$F_{zz} + F_{xx} - 1 \leq F_{process} \leq \text{Min}\{F_{zz}, F_{xx}\}. \quad (10)$$

Thus, we can estimate $0.73 \leq F_{process} \leq 0.86$. The process fidelity also benchmarks the minimal entanglement ca-

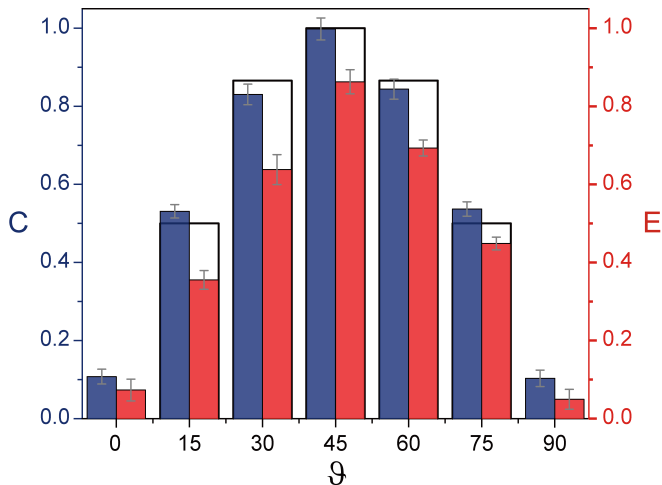


Figure 4. **Activation of entanglement from coherence.** The blue bars represent the measured coherence of system qubit as quantified by the ℓ_1 -norm of coherence in Eq. (8). The red bars represent the measured entanglement in the two-qubit state after the incoherent operation, quantified by the concurrence in Eq. (9). The outside frames are the theoretical prediction for coherence and entanglement. The experimental results show the same tendency as we vary the parameter ϑ . All error bars are estimated by the Monte Carlo simulation with 1000 rounds by assuming the Poissonian distribution of the photon statistics.

pability $C \geq 2F_{process} - 1$, as in our case, the result is larger than 0.47.

After experimentally characterizing the incoherent operation, we generate a series of quantum states:

$$\rho = \cos^2(\vartheta)|H\rangle\langle H| + \cos(\vartheta)\sin(\vartheta)|H\rangle\langle V| + \sin(\vartheta)\cos(\vartheta)|V\rangle\langle H| + \sin^2(\vartheta)|V\rangle\langle V| \quad (11)$$

By choosing different polarization parameter ϑ , we are able to tune the corresponding amount of coherence in the system qubit in $\{|H\rangle, |V\rangle\}$ basis. We split the system qubit on a beam splitter and prepare the two copies with the same polarization to test the relationship between coherence and entanglement. The ancilla qubit is fixed to $\sigma_i = |H\rangle\langle H|$ as an incoherent state during the whole experiment. We first conduct the one-qubit tomography with a combination of quarter wave plate and polarizer to reconstruct the 2×2 density matrix of the system qubit [39] and further estimate the amount of coherence defined in Eq. (8). The other copy of the system qubit is guided to the CNOT gate and interferes with the ancilla qubit on the PPBS. After the incoherent operation, the two-qubit tomography is used to evaluate the entanglement, as quantified via concurrence in Eq. (9).

In our experiment, we prepare seven different system states to test the relation between coherence and entanglement in Eq. (1). As we vary the coherence parameter, the density matrix of the entanglement states generated by the incoherent operation correspondingly

alter, as demonstrated in Fig. 3, from separable states to maximal entangled state. To further evaluate the relation between coherence and entanglement, we compare their exact values in Fig. 4. The blue bars represent the amount of coherence and the red bars represent the amount of entanglement. The outside frames are the theoretical prediction by considering the ideal cases.

With high-extinction polarization device, we are able to prepare the maximal coherence state $|D\rangle = (|H\rangle + |V\rangle)/\sqrt{2}$ and the measured coherence is up to $C = 0.999$, which is very close to ideal scenario. The measured entanglement of the generated entangled state is $E = 0.864$. In the next step we decrease the coherence of the system qubit and the corresponding entanglement changes with the same tendency. The system with the minimal coherence in our experiment has $C = 0.09$, and the corresponding activated entanglement between the two qubit is measured to be $E = 0.07$. Given the imperfection of the incoherent operation, certain mismatch exists between the measured entanglement and coherence. A considerably high conversion efficiency can be expected after certain optimization of the device.

CONCLUSIONS

In this work we explored the possibilities and limitation to activate entanglement from quantum coherence and superposition. While coherence can be activated into entanglement via free unitaries of the theory [20], we have shown that such an activation is not possible within a more general theory of quantum superposition. We have rigorously proven this statement for a general two-qubit system, where each of the qubits has two superposition-free states $|c_0\rangle$ and $|c_1\rangle$ with $0 < |\langle c_0|c_1\rangle| < 1$. We have further shown that only eight superposition-free unitaries are possible in this setting, and all of them can be represented in terms of two elementary operations.

An important consequence of our discussion is the finding that in the general framework of superposition considered here there is no unitary which corresponds to the action of a CNOT gate, i.e., which flips the state of the second qubit between $|c_0\rangle$ and $|c_1\rangle$ conditioned on the first qubit being in the state $|c_0\rangle$ or $|c_1\rangle$. Such a CNOT gate exists only in the more restricted resource theory of coherence, which arises in our framework in the limit of orthogonal states $|c_0\rangle$ and $|c_1\rangle$. These results are analogous to the no-cloning theorem [19], i.e., while it is not possible to clone a general quantum state, cloning is possible in a more restricted theory, where the considered states are mutually orthogonal.

We have experimentally demonstrated that entanglement activation from coherence is indeed possible. We have prepared single-qubit states with different values of coherence by using polarized photons and experi-

mentally activated coherence into entanglement via an optical CNOT gate which is the optimal incoherent operation in the considered setting. We have then compared the amount of final entanglement to the amount of initial coherence, finding a good agreement between theory and experiment. Both quantities clearly show the same tendency: a large amount of initial coherence leads to a large amount of activated entanglement.

We also note that related results have been presented very recently in [40], where cyclic interconversion between coherence and entanglement has been demonstrated experimentally, based on the framework of assisted coherence distillation [41, 42] and coherence activation from entanglement [20] and quantum discord [43, 44].

Our work also lead to a surprising result in entanglement theory, showing that the trace norm entanglement violates strong monotonicity. This solves an important question in quantum information theory which was open for decades, and clearly demonstrate how recent developments on the resource theory of quantum coherence [4] can be applied for advancing other research areas of quantum information and technology.

METHODS

An important question in any quantum resource theory is to quantify the amount of the resource in a given quantum state. A general resource quantifier \mathcal{R} should at least have the following property:

$$\mathcal{R}(\Lambda_f[\rho]) \leq \mathcal{R}(\rho), \quad (12)$$

where Λ_f is a free operation of the resource theory. In entanglement theory, Λ_f are usually chosen to be *local operations and classical communication* [3]. In the resource theory of coherence, a possible choice for Λ_f are *incoherent operations* introduced in [6], and alternative frameworks have also been discussed recently [45, 46], see also the review [4] and references therein.

Any nonnegative function \mathcal{R} which fulfills Eq. (12) is called *monotone* of the corresponding resource theory. A very general family are distance-based monotones

$$\mathcal{R}_D(\rho) = \inf_{\sigma \in \mathcal{F}} D(\rho, \sigma), \quad (13)$$

where \mathcal{F} is the set of free states and D is a suitable distance. The quantity \mathcal{R}_D fulfills monotonicity (12) for any distance D which is contractive under quantum operations: $D(\Lambda[\rho], \Lambda[\sigma]) \leq D(\rho, \sigma)$. Important examples for such distances are the quantum relative entropy $S(\rho\|\sigma) = \text{Tr}[\rho \log_2 \rho] - \text{Tr}[\rho \log_2 \sigma]$ and the trace distance $D_t(\rho, \sigma) = \frac{1}{2} \|\rho - \sigma\|_1$ with the trace norm $\|M\|_1 = \text{Tr} \sqrt{M^\dagger M}$.

In many resource theories it is also important to consider *selective free operations*. Here, an initial quantum state ρ is transformed into an ensemble

$$\rho \rightarrow \{q_i, \sigma_i\} \quad (14)$$

with probabilities q_i and quantum states σ_i . In entanglement theory, this is motivated by the fact that the parties can – in principle – record the outcome of their local measurements. Each state σ_i then corresponds to the state of the system for a particular sequence of local measurement outcomes, with a corresponding overall probability q_i . A similar approach has been taken recently in the resource theory of coherence [4, 6, 45, 46].

For a resource theory with selective free operations as given in Eq. (14), it is reasonable to demand that the corresponding resource quantifier \mathcal{R} admits *strong monotonicity*:

$$\sum_i q_i \mathcal{R}(\sigma_i) \leq \mathcal{R}(\rho) \quad (15)$$

for any ensemble $\{q_i, \sigma_i\}$ which can be obtained from the state ρ by the means of selective free operations. The motivation for this requirement is similar to the standard monotonicity (12): the resource should not increase on average even if the outcomes of free measurements are recorded. Entanglement and coherence monotones based on the relative entropy fulfill strong monotonicity [5, 6]. As was shown in [28], the trace norm coherence violates strong monotonicity. As we prove in Appendix B, strong monotonicity is also violated by the trace norm entanglement. Note that strong monotonicity (15) implies monotonicity (12) if \mathcal{R} is convex.

ACKNOWLEDGEMENTS

We acknowledge discussion with P. Horodecki and J.-W. Pan. This work was supported by National Key R&D Program of China (2017YFA0303700), National Natural Science Foundation of China (NSFC) (11374211, 11690033, 11275131, 11571313), Shanghai Municipal Education Commission (SMEC)(16SG09, 2017-01-07-00-02-E00049), Science and Technology Commission of Shanghai Municipality (STCSM) (15QA1402200, 16JC1400405) and Open fund from HPCL (201511-01). X.-M.J. acknowledges support from the National Young 1000 Talents Plan. A.S. was supported by the National Science Center in Poland (POLONEZ UMO-2016/21/P/ST2/04054). S.R. and M.L. acknowledge support from EC grants OSYRIS (ERC-2013-ADG No. 339106) and QUIC (H2020-FETPROACT-2014 No. 641122), the Spanish MINECO grants Severo Ochoa (SEV-2015-0522), FISICATEAMO (FIS2016-79508-P), MINECO CLUSTER (ICFO15-EE-3785), the Generalitat de Catalunya (2014 SGR 874 and 5 CERCA/Program) and the Fundació Privada Cellex.

* These authors contributed equally to this work.

† xianmin.jin@sjtu.edu.cn

- [1] E. Schrödinger, *Naturwissenschaften* **23**, 807 (1935).
- [2] A. Einstein, B. Podolsky, and N. Rosen, *Phys. Rev.* **47**, 777 (1935).
- [3] R. Horodecki, P. Horodecki, M. Horodecki, and K. Horodecki, *Rev. Mod. Phys.* **81**, 865 (2009).
- [4] A. Streltsov, G. Adesso, and M. B. Plenio, *arXiv:1609.02439* (2016).
- [5] V. Vedral, M. B. Plenio, M. A. Rippin, and P. L. Knight, *Phys. Rev. Lett.* **78**, 2275 (1997).
- [6] T. Baumgratz, M. Cramer, and M. B. Plenio, *Phys. Rev. Lett.* **113**, 140401 (2014).
- [7] R. F. Werner, *Phys. Rev. A* **40**, 4277 (1989).
- [8] C. H. Bennett, G. Brassard, C. Crépeau, R. Jozsa, A. Peres, and W. K. Wootters, *Phys. Rev. Lett.* **70**, 1895 (1993).
- [9] X.-M. Jin, J.-G. Ren, B. Yang, Z.-H. Yi, F. Zhou, X.-F. Xu, S.-K. Wang, D. Yang, Y.-F. Hu, S. Jiang, T. Yang, H. Yin, K. Chen, C.-Z. Peng, and J.-W. Pan, *Nat. Photon.* **4**, 376 (2010).
- [10] A. K. Ekert, *Phys. Rev. Lett.* **67**, 661 (1991).
- [11] M. Horodecki, J. Oppenheim, and A. Winter, *Nature* **436**, 673 (2005).
- [12] J. Yin, Y. Cao, Y.-H. Li, S.-K. Liao, L. Zhang, J.-G. Ren, W.-Q. Cai, W.-Y. Liu, B. Li, H. Dai, G.-B. Li, Q.-M. Lu, Y.-H. Gong, Y. Xu, S.-L. Li, F.-Z. Li, Y.-Y. Yin, Z.-Q. Jiang, M. Li, J.-J. Jia, G. Ren, D. He, Y.-L. Zhou, X.-X. Zhang, N. Wang, X. Chang, Z.-C. Zhu, N.-L. Liu, Y.-A. Chen, C.-Y. Lu, R. Shu, C.-Z. Peng, J.-Y. Wang, and J.-W. Pan, *Science* **35**, 1140 (2017).
- [13] W. H. Zurek, *Rev. Mod. Phys.* **75**, 715 (2003).
- [14] V. Giovannetti, S. Lloyd, and L. Maccone, *Nat. Photon.* **5**, 222 (2011).
- [15] I. Marvian and R. W. Spekkens, *Phys. Rev. A* **94**, 052324 (2016).
- [16] M. Hillery, *Phys. Rev. A* **93**, 012111 (2016).
- [17] J. M. Matera, D. Egloff, N. Killoran, and M. B. Plenio, *Quantum Sci. Technol.* **1**, 01LT01 (2016).
- [18] S. Huelga and M. Plenio, *Contemporary Physics* **54**, 181 (2013).
- [19] W. K. Wootters and W. H. Zurek, *Nature* **299**, 802 (1982).
- [20] A. Streltsov, U. Singh, H. S. Dhar, M. N. Bera, and G. Adesso, *Phys. Rev. Lett.* **115**, 020403 (2015).
- [21] N. Killoran, F. E. S. Steinhoff, and M. B. Plenio, *Phys. Rev. Lett.* **116**, 080402 (2016).
- [22] T. Theurer, N. Killoran, D. Egloff, and M. B. Plenio, *arXiv:1703.10943* (2017).
- [23] I. Marvian and R. W. Spekkens, *New J. Phys.* **15**, 033001 (2013).
- [24] A. Chefles, R. Jozsa, and A. Winter, *Int. J. Quant. Inf.* **2**, 11 (2004).
- [25] B. Regula, M. Piani, M. Cianciaruso, T. R. Bromley, A. Streltsov, and G. Adesso, *arXiv:1704.04153* (2017).
- [26] S. Rana, P. Parashar, and M. Lewenstein, *Phys. Rev. A* **93**, 012110 (2016).
- [27] J. Chen, S. Grogan, N. Johnston, C.-K. Li, and S. Plosker, *Phys. Rev. A* **94**, 042313 (2016).
- [28] X.-D. Yu, D.-J. Zhang, G. F. Xu, and D. M. Tong, *Phys. Rev. A* **94**, 060302 (2016).
- [29] J. Eisert, *Entanglement in quantum information theory*, Ph.D. thesis, University of Potsdam (2001), *arXiv:quant-ph/0610253*.
- [30] W. K. Wootters, *Phys. Rev. Lett.* **80**, 2245 (1998).
- [31] L.-H. Shao, Z. Xi, H. Fan, and Y. Li, *Phys. Rev. A* **91**, 042120 (2015).
- [32] N. Kiesel, C. Schmid, U. Weber, R. Ursin, and H. Weinfurter, *Phys. Rev. Lett.* **95**, 210505 (2005).
- [33] R. Okamoto, H. F. Hofmann, S. Takeuchi, and K. Sasaki, *Phys. Rev. Lett.* **95**, 210506 (2005).
- [34] A. Crespi, R. Ramponi, R. Osellame, L. Sansoni, I. Bongioanni, F. Sciarrino, G. Vallone, and P. Mataloni, *Nature Commun.* **2**, 566 (2011).
- [35] Y.-H. Kim, *Phys. Rev. A* **68**, 013804 (2003).
- [36] P. G. Kwiat, K. Mattle, H. Weinfurter, A. Zeilinger, A. V. Sergienko, and Y. Shih, *Phys. Rev. Lett.* **75**, 4337 (1995).
- [37] C. K. Hong, Z. Y. Ou, and L. Mandel, *Phys. Rev. Lett.* **59**, 2044 (1987).
- [38] H. F. Hofmann, *Phys. Rev. Lett.* **94**, 160504 (2005).
- [39] D. F. V. James, P. G. Kwiat, W. J. Munro, and A. G. White, *Phys. Rev. A* **64**, 052312 (2001).
- [40] K.-D. Wu, Z. Hou, Y.-Y. Zhao, G.-Y. Xiang, C.-F. Li, G.-C. Guo, J. Ma, Q.-Y. He, J. Thompson, and M. Gu, *arXiv:1710.01738* (2017).
- [41] E. Chitambar, A. Streltsov, S. Rana, M. N. Bera, G. Adesso, and M. Lewenstein, *Phys. Rev. Lett.* **116**, 070402 (2016).
- [42] A. Streltsov, S. Rana, M. N. Bera, and M. Lewenstein, *Phys. Rev. X* **7**, 011024 (2017).
- [43] K. Modi, A. Brodutch, H. Cable, T. Paterek, and V. Vedral, *Rev. Mod. Phys.* **84**, 1655 (2012).
- [44] J. Ma, B. Yadin, D. Girolami, V. Vedral, and M. Gu, *Phys. Rev. Lett.* **116**, 160407 (2016).
- [45] A. Winter and D. Yang, *Phys. Rev. Lett.* **116**, 120404 (2016).
- [46] B. Yadin, J. Ma, D. Girolami, M. Gu, and V. Vedral, *Phys. Rev. X* **6**, 041028 (2016).
- [47] T.-C. Wei and P. M. Goldbart, *Phys. Rev. A* **68**, 042307 (2003).
- [48] A. Streltsov, H. Kampermann, and D. Bruß, *New J. Phys.* **12**, 123004 (2010).

Appendix A: Proof of Theorem 2

In the following, we will characterize all superposition-free unitaries acting on two qubits. In particular, we will show that any superposition-free unitary in this framework can be decomposed into a sequence of elementary unitaries V and W , given in Eqs. (3) and (4) of the main text. An important ingredient for our proof is the following lemma [21, 23, 24].

Lemma 4. *For two sets of states $\{|\psi_i\rangle\}_{i=1}^N$ and $\{|\phi_i\rangle\}_{i=1}^N$ there exists a unitary operation such that $U|\psi_i\rangle = |\phi_i\rangle$ for all i if and only if $\langle\psi_i|\psi_j\rangle = \langle\phi_i|\phi_j\rangle$ holds true for all i and j .*

In general, a superposition-free unitary U acts on a superposition-free state $|c_k\rangle|c_l\rangle$ as follows:

$$U|c_k\rangle|c_l\rangle = e^{i\phi_{kl}}|c_m\rangle|c_n\rangle, \quad (\text{A1})$$

where the possible final states $e^{i\phi_{kl}}|c_m\rangle|c_n\rangle$ are constrained by Lemma 4. As we will see in the following, there exist 8 classes of superposition-free unitaries. For

each of those classes we will find a decomposition into the elementary operations V and W .

Class 1. We start with the most simple transformation, corresponding to the situation where an initial superposition-free state remains unchanged (up to a possible phase):

$$|c_0\rangle |c_0\rangle \rightarrow e^{i\phi_{00}} |c_0\rangle |c_0\rangle, \quad (\text{A2a})$$

$$|c_1\rangle |c_1\rangle \rightarrow e^{i\phi_{11}} |c_1\rangle |c_1\rangle, \quad (\text{A2b})$$

$$|c_0\rangle |c_1\rangle \rightarrow e^{i\phi_{01}} |c_0\rangle |c_1\rangle, \quad (\text{A2c})$$

$$|c_1\rangle |c_0\rangle \rightarrow e^{i\phi_{10}} |c_1\rangle |c_0\rangle. \quad (\text{A2d})$$

Note that by Lemma 4, all phases $e^{i\phi_{kl}}$ must be equal. It is straightforward to see that this transformation corresponds to V^2 .

Class 2. We now consider the transformation

$$|c_0\rangle |c_0\rangle \rightarrow e^{i\phi_{00}} |c_0\rangle |c_0\rangle, \quad (\text{A3a})$$

$$|c_1\rangle |c_1\rangle \rightarrow e^{i\phi_{11}} |c_1\rangle |c_1\rangle, \quad (\text{A3b})$$

$$|c_0\rangle |c_1\rangle \rightarrow e^{i\phi_{01}} |c_1\rangle |c_0\rangle, \quad (\text{A3c})$$

$$|c_1\rangle |c_0\rangle \rightarrow e^{i\phi_{10}} |c_0\rangle |c_1\rangle. \quad (\text{A3d})$$

By applying Lemma 4, we see that – similar as in the previous case – all phases $e^{i\phi_{kl}}$ must be equal. This transformation corresponds to the swap unitary V .

Class 3. The next transformation that we will consider has the following form:

$$|c_0\rangle |c_0\rangle \rightarrow e^{i\phi_{00}} |c_1\rangle |c_1\rangle, \quad (\text{A4a})$$

$$|c_1\rangle |c_1\rangle \rightarrow e^{i\phi_{11}} |c_0\rangle |c_0\rangle, \quad (\text{A4b})$$

$$|c_0\rangle |c_1\rangle \rightarrow e^{i\phi_{01}} |c_0\rangle |c_1\rangle, \quad (\text{A4c})$$

$$|c_1\rangle |c_0\rangle \rightarrow e^{i\phi_{10}} |c_1\rangle |c_0\rangle. \quad (\text{A4d})$$

Up to an overall phase, the phases $e^{i\phi_{kl}}$ are fixed by Lemma 4 as follows:

$$e^{i\phi_{00}} = 1, \quad (\text{A5a})$$

$$e^{i\phi_{01}} = e^{i\phi_{10}} = e^{i\frac{\phi_{11}}{2}} = \frac{\langle c_0|c_1\rangle}{\langle c_1|c_0\rangle}. \quad (\text{A5b})$$

This transformation corresponds to the unitary WVW .

Class 4. In the next step we consider the following transformation:

$$|c_0\rangle |c_0\rangle \rightarrow e^{i\phi_{00}} |c_1\rangle |c_1\rangle, \quad (\text{A6a})$$

$$|c_1\rangle |c_1\rangle \rightarrow e^{i\phi_{11}} |c_0\rangle |c_0\rangle, \quad (\text{A6b})$$

$$|c_0\rangle |c_1\rangle \rightarrow e^{i\phi_{01}} |c_1\rangle |c_0\rangle, \quad (\text{A6c})$$

$$|c_1\rangle |c_0\rangle \rightarrow e^{i\phi_{10}} |c_0\rangle |c_1\rangle. \quad (\text{A6d})$$

It can be verified by inspection that (up to an overall phase), Lemma 4 fixes the phases $e^{i\phi_{kl}}$ in the same way as in Eq. (A5). Note that this transformation corresponds to the transformation of Class 3, followed by a swap. Thus, it corresponds to the unitary $(VW)^2$.

Class 5. We now consider the transformation

$$|c_0\rangle |c_0\rangle \rightarrow e^{i\phi_{00}} |c_1\rangle |c_0\rangle, \quad (\text{A7a})$$

$$|c_1\rangle |c_1\rangle \rightarrow e^{i\phi_{11}} |c_0\rangle |c_1\rangle, \quad (\text{A7b})$$

$$|c_0\rangle |c_1\rangle \rightarrow e^{i\phi_{01}} |c_1\rangle |c_1\rangle, \quad (\text{A7c})$$

$$|c_1\rangle |c_0\rangle \rightarrow e^{i\phi_{10}} |c_0\rangle |c_0\rangle. \quad (\text{A7d})$$

Up to an overall phase, Lemma 4 fixes the phases $e^{i\phi_{kl}}$ as follows:

$$e^{i\phi_{00}} = e^{i\phi_{01}} = 1, \quad (\text{A8a})$$

$$e^{i\phi_{11}} = e^{i\phi_{10}} = \frac{\langle c_0|c_1\rangle}{\langle c_1|c_0\rangle}. \quad (\text{A8b})$$

This transformation corresponds to the unitary W .

Class 6. In the next step we consider the transformation

$$|c_0\rangle |c_0\rangle \rightarrow e^{i\phi_{00}} |c_1\rangle |c_0\rangle, \quad (\text{A9a})$$

$$|c_1\rangle |c_1\rangle \rightarrow e^{i\phi_{11}} |c_0\rangle |c_1\rangle, \quad (\text{A9b})$$

$$|c_0\rangle |c_1\rangle \rightarrow e^{i\phi_{01}} |c_0\rangle |c_0\rangle, \quad (\text{A9c})$$

$$|c_1\rangle |c_0\rangle \rightarrow e^{i\phi_{10}} |c_1\rangle |c_1\rangle. \quad (\text{A9d})$$

By applying Lemma 4, we see that the phases $e^{i\phi_{kl}}$ are fixed as follows:

$$e^{i\phi_{00}} = e^{i\phi_{10}} = 1, \quad (\text{A10a})$$

$$e^{i\phi_{11}} = e^{i\phi_{01}} = \frac{\langle c_0|c_1\rangle}{\langle c_1|c_0\rangle}. \quad (\text{A10b})$$

As can be verified by inspection, this transformation corresponds to the unitary WV .

Class 7. The next transformation that we will consider has the following form:

$$|c_0\rangle |c_0\rangle \rightarrow e^{i\phi_{00}} |c_0\rangle |c_1\rangle, \quad (\text{A11a})$$

$$|c_1\rangle |c_1\rangle \rightarrow e^{i\phi_{11}} |c_1\rangle |c_0\rangle, \quad (\text{A11b})$$

$$|c_0\rangle |c_1\rangle \rightarrow e^{i\phi_{01}} |c_0\rangle |c_0\rangle, \quad (\text{A11c})$$

$$|c_1\rangle |c_0\rangle \rightarrow e^{i\phi_{10}} |c_1\rangle |c_1\rangle. \quad (\text{A11d})$$

Up to an overall phase, Lemma 4 fixes the phases $e^{i\phi_{kl}}$ as in Eqs. (A10). This transformation corresponds to the transformation of Class 6 followed by a swap, and the corresponding unitary is VWV .

Class 8. Our final transformation has the following form:

$$|c_0\rangle |c_0\rangle \rightarrow e^{i\phi_{00}} |c_0\rangle |c_1\rangle, \quad (\text{A12a})$$

$$|c_1\rangle |c_1\rangle \rightarrow e^{i\phi_{11}} |c_1\rangle |c_0\rangle, \quad (\text{A12b})$$

$$|c_0\rangle |c_1\rangle \rightarrow e^{i\phi_{01}} |c_1\rangle |c_1\rangle, \quad (\text{A12c})$$

$$|c_1\rangle |c_0\rangle \rightarrow e^{i\phi_{10}} |c_0\rangle |c_0\rangle. \quad (\text{A12d})$$

Up to an overall phase, Lemma 4 fixes the phases $e^{i\phi_{kl}}$ as in Eq. (A8). This transformation corresponds to the

transformation of Class 5 followed by a swap, and the corresponding unitary is VW .

As we will discuss in the following, these eight classes indeed characterize all superposition-free unitaries on two qubits. This can be seen by inspection, applying Lemma 4 to all the remaining permutations of the superposition-free states. As an example, consider the following transition:

$$|c_0\rangle|c_0\rangle \rightarrow e^{i\phi_{00}} |c_0\rangle|c_0\rangle, \quad (\text{A13a})$$

$$|c_1\rangle|c_1\rangle \rightarrow e^{i\phi_{11}} |c_1\rangle|c_0\rangle, \quad (\text{A13b})$$

$$|c_0\rangle|c_1\rangle \rightarrow e^{i\phi_{01}} |c_0\rangle|c_1\rangle, \quad (\text{A13c})$$

$$|c_1\rangle|c_0\rangle \rightarrow e^{i\phi_{10}} |c_1\rangle|c_1\rangle. \quad (\text{A13d})$$

Transition of this form can be regarded as CNOT operation in the resource theory of superposition, as (up to a phase) the state of the second qubit is flipped between $|c_0\rangle$ and $|c_1\rangle$, conditioned on the first qubit being in one of these states.

The transition in Eqs. (A13) is not covered by the above classes, and it is indeed impossible via unitary operations. If such a transition was possible via unitaries, this would lead to a violation of Lemma 4. In particular, Lemma 4 together with Eqs. (A13a) and (A13b) implies that

$$\langle c_0|c_1\rangle^2 = e^{i(\phi_{11}-\phi_{00})} \langle c_0|c_1\rangle, \quad (\text{A14})$$

which cannot be true for any choice of the phases $e^{i\phi_{00}}$ and $e^{i\phi_{11}}$ in the considered range $0 < |\langle c_0|c_1\rangle| < 1$. By similar arguments, all transitions which are not covered by the above classes can be ruled out, and the proof is complete.

Appendix B: Proof of Theorem 3

In the following, we will use results from [27], where the authors provided an important link between E_t and C_t . In particular, theorems 2 and 3 in [27] imply the following equality:

$$E_t \left(\frac{1}{d} \sum_{i,j=0}^{d-1} |ii\rangle\langle jj| \right) = C_t \left(\frac{1}{d} \sum_{i,j=0}^{d-1} |i\rangle\langle j| \right) = 2 - \frac{2}{d}. \quad (\text{B1})$$

Equipped with these tools we are now in position to prove Theorem 3 of the main text.

We will consider the bipartite state

$$\rho = \frac{p}{2} \sum_{i,j=0}^1 |ii\rangle\langle jj| + \frac{1-p}{3} \sum_{k,l=2}^4 |kk\rangle\langle ll| \quad (\text{B2})$$

with probability $0 \leq p \leq 1$. Consider now local measurement on the first party with Kraus operators

$$K_1 = \sum_{i=0}^1 |i\rangle\langle i| \otimes \mathbb{1}, \quad K_2 = \sum_{j=2}^4 |j\rangle\langle j| \otimes \mathbb{1}. \quad (\text{B3})$$

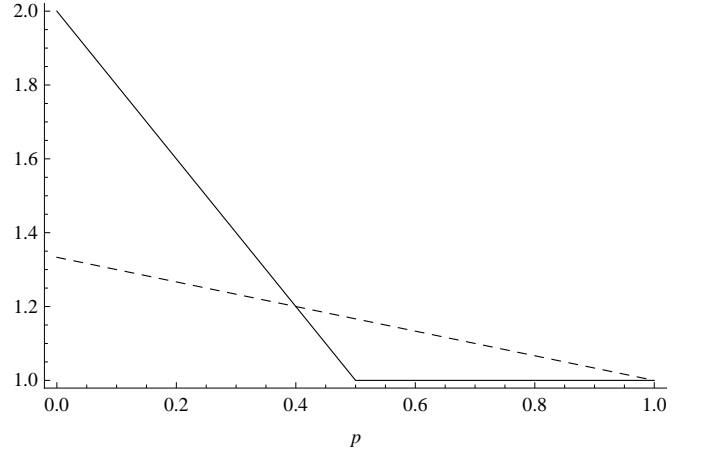


Figure 5. Violation of strong monotonicity of trace norm entanglement for the state ρ given in Eq. (B2). Solid line shows an upper bound on the trace norm entanglement of ρ . Dashed line shows the average entanglement $q_1 E_t(\sigma_1) + q_2 E_t(\sigma_2)$ after a suitable local measurement. Violation of strong monotonicity is obtained in the range $0.4 < p < 1$.

It is straightforward to check that the corresponding measurement probabilities take the form

$$q_1 = \text{Tr}[K_1 \rho K_1^\dagger] = p, \quad (\text{B4})$$

$$q_2 = \text{Tr}[K_2 \rho K_2^\dagger] = 1 - p. \quad (\text{B5})$$

Moreover, the post-measurement states are given as

$$\sigma_1 = \frac{K_1 \rho K_1^\dagger}{p_1} = \frac{1}{2} \sum_{i,j=0}^1 |ii\rangle\langle jj|, \quad (\text{B6})$$

$$\sigma_2 = \frac{K_2 \rho K_2^\dagger}{p_2} = \frac{1}{3} \sum_{k,l=2}^4 |kk\rangle\langle ll|. \quad (\text{B7})$$

We will now complete the proof of the theorem by showing that for a suitable choice of the probability p it holds that

$$q_1 E_t(\sigma_1) + q_2 E_t(\sigma_2) > E_t(\rho). \quad (\text{B8})$$

For this, we define the separable state $\delta = \frac{1}{2} \sum_{i=0}^1 |ii\rangle\langle ii|$, and note that it provides an upper bound on the trace norm entanglement, i.e., $E_t(\rho) \leq \|\rho - \delta\|_1$. Moreover, it is straightforward to verify that

$$\|\rho - \delta\|_1 = \begin{cases} 2 - 2p & \text{for } p < \frac{1}{2}, \\ 1 & \text{for } p \geq \frac{1}{2}. \end{cases} \quad (\text{B9})$$

On the other hand, using Eq. (B1) we obtain

$$E_t(\sigma_1) = 1, \quad E_t(\sigma_2) = \frac{4}{3}. \quad (\text{B10})$$

Using these results, we immediately see that Eq. (B8) is fulfilled for $0.4 < p < 1$, see also Fig. 5.

Appendix C: Activation of ℓ_1 -norm coherence into concurrence

We will now show that the inequality

$$E(\Lambda_i[\rho \otimes \sigma_i]) \leq C(\rho) \quad (\text{C1})$$

holds for ℓ_1 -norm coherence C and concurrence E , where ρ and σ_i are single-qubit states, and Λ_i is a bipartite incoherent operation. Moreover, we will also see that equality in Eq. (C1) is achieved if Λ_i is a CNOT gate.

For proving the statement, we first recall the definition of geometric entanglement [47, 48] and geometric coherence [20]

$$E_g(\rho) = 1 - \max_{\sigma \in \mathcal{S}} F(\rho, \sigma), \quad (\text{C2})$$

$$C_g(\rho) = 1 - \max_{\sigma \in \mathcal{I}} F(\rho, \sigma) \quad (\text{C3})$$

with fidelity $F(\rho, \sigma) = \|\sqrt{\rho} \sqrt{\sigma}\|_1^2$. Note that these quantities fulfill Eq. (C1), and equality is attained if Λ_i is a CNOT gate [20].

For a single-qubit state ρ , the geometric coherence C_g is related to the ℓ_1 -norm coherence C as follows [20]:

$$C_g(\rho) = \frac{1}{2}[1 - \sqrt{1 - C(\rho)^2}]. \quad (\text{C4})$$

It is now crucial to note that the same functional relation holds between the geometric entanglement E_g and the concurrence E for any two-qubit state μ [47, 48]:

$$E_g(\mu) = \frac{1}{2}[1 - \sqrt{1 - E(\mu)^2}]. \quad (\text{C5})$$

Recalling that Eq. (C1) is fulfilled for the geometric entanglement E_g and geometric coherence C_g , these results imply that Eq. (C1) also holds for ℓ_1 -norm of coherence C and concurrence E . Moreover, for these quantifiers the CNOT gate must also be the optimal incoherent operation, attaining equality in Eq. (C1). Our results also hold if C is chosen to be the trace norm coherence, as for single-qubit states the trace norm coherence coincided with the ℓ_1 -norm coherence [31].